

## Electronic properties of a C N x thin films: An x-ray-absorption and photoemission spectroscopy study

S. C. Ray, C. W. Pao, J. W. Chiou, H. M. Tsai, J. C. Jan, W. F. Pong, R. McCann, S. S. Roy, P. Papakonstantinou, and J. A. McLaughlin

Citation: *Journal of Applied Physics* **98**, 033708 (2005); doi: 10.1063/1.1994933

View online: <http://dx.doi.org/10.1063/1.1994933>

View Table of Contents: <http://scitation.aip.org/content/aip/journal/jap/98/3?ver=pdfcov>

Published by the [AIP Publishing](#)

---

### Articles you may be interested in

Electronic states of NO<sub>2</sub>-exposed H-terminated diamond/Al<sub>2</sub>O<sub>3</sub> heterointerface studied by synchrotron radiation photoemission and X-ray absorption spectroscopy

*Appl. Phys. Lett.* **104**, 072101 (2014); 10.1063/1.4865929

Enhancement of Si–O hybridization in low-temperature grown ultraviolet photo-oxidized Si O<sub>2</sub> film observed by x-ray absorption and photoemission spectroscopy

*J. Appl. Phys.* **103**, 013704 (2008); 10.1063/1.2828144

Bonding properties and their relation to residual stress and refractive index of amorphous Ta(N,O) films investigated by x-ray absorption spectroscopy

*Appl. Phys. Lett.* **86**, 161910 (2005); 10.1063/1.1905784

Threshold of photoelectron emission from C N x films deposited at room temperature and at 500 ° C

*J. Appl. Phys.* **96**, 4674 (2004); 10.1063/1.1787907

Electronic and bonding structures of B-C-N thin films investigated by x-ray absorption and photoemission spectroscopy

*J. Appl. Phys.* **96**, 208 (2004); 10.1063/1.1759392

---



**2014 Special Topics**

PEROVSKITES | 2D MATERIALS | MESOPOROUS MATERIALS | BIOMATERIALS/ BIOELECTRONICS | METAL-ORGANIC FRAMEWORK MATERIALS

**AIP** | APL Materials

**Submit Today!**

# Electronic properties of $a\text{-CN}_x$ thin films: An x-ray-absorption and photoemission spectroscopy study

S. C. Ray,<sup>a)</sup> C. W. Pao, J. W. Chiou, H. M. Tsai, J. C. Jan, and W. F. Pong  
*Department of Physics, Tamkang University, Tamsui, Taiwan 251, Republic of China*

R. McCann, S. S. Roy, P. Papakonstantinou, and J. A. McLaughlin  
*Nanotechnology Research Institute (NRI), School of Electrical and Mechanical Engineering,  
 University of Ulster at Jordanstown, Newtownabbey, County Antrim BT37 0QB, Northern Ireland*

(Received 17 March 2005; accepted 15 June 2005; published online 8 August 2005)

The electronic properties of amorphous carbon nitride were studied by x-ray-absorption near-edge structure (XANES) and valence-band photoelectron spectroscopy (PES). The nitrogen incorporation was found to induce graphitization, as evidenced by an increase of the  $sp^2$  cluster in C and N  $K$ -edge XANES spectra. The structure is found to be similar to pyridine. Hybridized C–N bond lengths were determined from the position of the  $\sigma^*$  resonance of XANES spectra and the obtained results suggest  $sp^2$  hybridization. A valence-band PES spectrum showed that the  $p$ - $\pi$  band became more intense than the  $p$ - $\sigma$  band upon higher at. % nitrogen addition, which confirmed the role played by the  $\pi$  bonds in controlling the electronic structure of  $a\text{-CN}_x$  films. © 2005 American Institute of Physics. [DOI: 10.1063/1.1994933]

## I. INTRODUCTION

Motivated by the theoretical work of Liu and Cohen,<sup>1</sup> proposing a hypothetical compound  $\beta\text{-C}_3\text{N}_4$  with a bulk modulus greater than that of a diamond, many attempts have been made in order to obtain carbon nitride with excellent mechanical properties. In spite of the lack of success in growing continuous films of the  $\beta\text{-C}_3\text{N}_4$  phase, it has been found that amorphous carbon nitride ( $a\text{-CN}_x$ ) presents attractive properties such as high hardness, low friction coefficient, and chemical inertness.<sup>2</sup> Different diffraction techniques have been used to characterize  $a\text{-CN}_x$  films. Yet, the atomic structure of amorphous carbon nitride is still very poorly known. This is mainly due to the rich variety of possible local environments and the lack of long-range order. Among the different techniques, the most promising one for the study of  $a\text{-CN}_x$  films is x-ray-absorption near-edge structure (XANES) spectroscopy. Very few reports<sup>3–5</sup> have been published on the characterization of  $a\text{-CN}_x$  films that make use of XANES spectroscopy and/or valence-band photoelectron spectroscopy (PES). In this work we have used C and N  $K$ -edge XANES and valence-band PES spectra to study the electronic properties of  $a\text{-CN}_x$  thin films deposited by pulsed laser deposition (PLD).

## II. EXPERIMENTAL DETAILS

The  $a\text{-CN}_x$  thin films were deposited on a Si (100) substrate at different nitrogen pressures by the PLD method. Details of the sample preparation are given elsewhere.<sup>6</sup> The XANES spectra of C and N  $K$ -edge spectra were performed using the high-energy spherical grating monochromator (HSGM) beam line, whereas the valence-band PES spectra were performed using the low-energy spherical grating

monochromator (LSGM) beam line with an electron-beam energy of 1.5 GeV and a maximum stored current of 200 mA at the National Synchrotron Radiation Research Center (NSRRC), Hsinchu, Taiwan. The XANES data of the C  $K$  edge were collected in the total yield mode by recording the sample drain current mode whereas the N  $K$  edge in the fluorescence mode using a seven-element Ge detector. Following preedge background subtraction, the spectra were normalized using the incident-beam intensity  $I_0$  and by keeping the area under the spectra in the energy range between 315 and 330 eV for the C  $K$  edge and 440–455 eV (not shown in figure) for the N  $K$  edge fixed. Valence-band PES spectra were obtained at an excitation of 100 eV having the typical resolution of 0.05–0.10 eV. The base pressure of  $\sim 5 \times 10^{-10}$  Torr was used during the measurements, which has an EAC-125 hemispherical electron energy analyzer. The samples were cleaned by repeated cycles of argon-ion bombardment before the measurements. All measurements of XANES as well as valence-band PES were taken at room temperature.

## III. RESULTS AND DISCUSSION

The XANES spectra of C and N  $K$  edges of an  $a\text{-CN}_x$  film are presented in Figs. 1 and 2, respectively. The graphite spectra are also plotted with C  $K$ -edge XANES spectra in Fig. 1(a) as a reference. In the C  $K$ -edge XANES spectra two prominent peaks at  $\sim 285.3(\pm 0.1)$  and  $\sim 286.8$  eV and a shoulder  $\sim 283.8$  eV are observed in the  $\pi^*$  region. This  $\pi^*$  region is clearly shown in the left inset of Fig. 1(a), after subtracting a Gaussian line, within the range of 281–289 eV. The peak at  $\sim 283.8$  eV is quite prominent [see left inset of Fig. 1(a)] at low nitrogen concentration (sample No. C14) and the peak position is gradually shifted towards higher energies with an increase of nitrogen concentration. The peak maximum at about 285.5 eV corresponds to the lowest-lying state of  $\pi$  symmetry  $\pi_0$ , near  $Q$  in the Brillouin zone of

<sup>a)</sup>Author to whom correspondence should be addressed; electronic mail: raysekhar@rediffmail.com

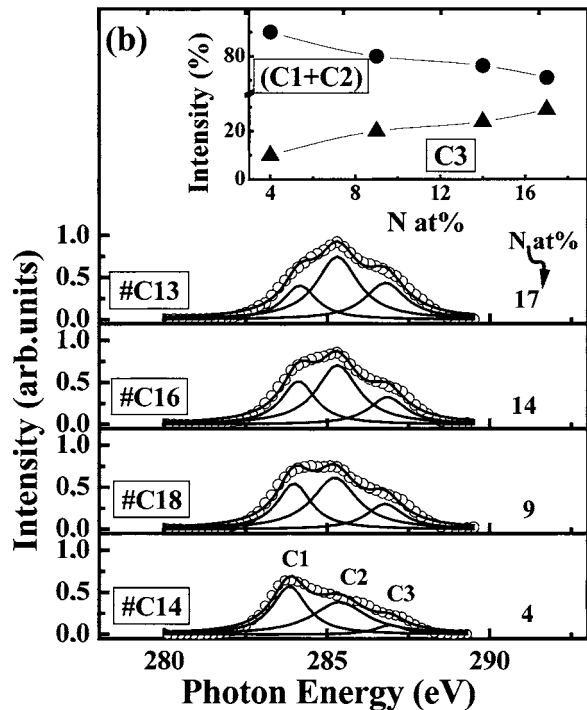
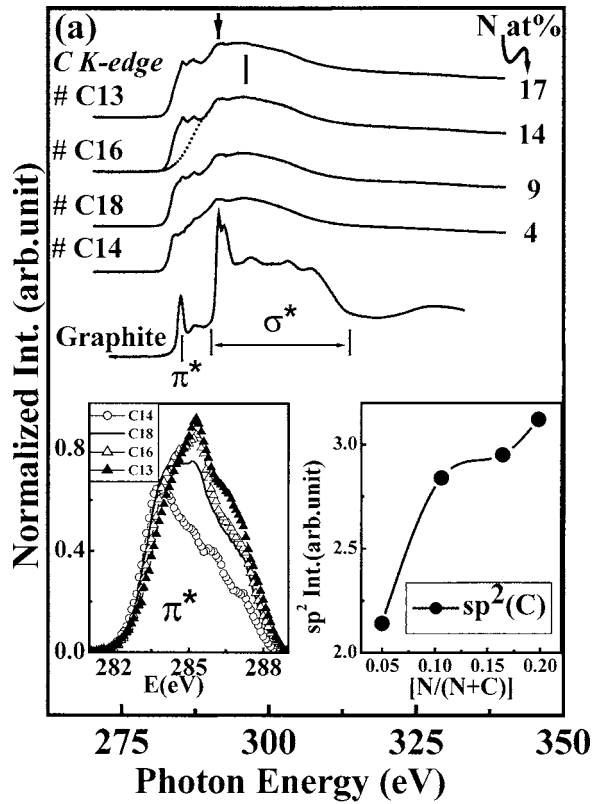


FIG. 1. (a) Normalized C *K*-edge absorption spectra of the *a*-CN<sub>x</sub> films. The inset shows the  $\pi^*$  region after subtraction using a Gaussian line and  $sp^2$  intensity variation with nitrogen content. (b) Decomposed  $\pi^*$  region of the C *K* edge into three peaks and their intensity variation with nitrogen content.

graphite.<sup>7</sup> The  $\pi^*$  antibonding state or white band for graphite is located at 285.3 eV and it originates from the out-of-plane bonds in the  $sp^2$  bonding configuration.<sup>8</sup> The peak at about  $\sim$ 284.0 eV (prepeak) is also found at the C *K* edge of a natural diamond, due to the presence of  $sp^2$ -bonded carbon.<sup>8</sup> Apart from the above two peaks at 284.0( $\pm$ 0.2) and

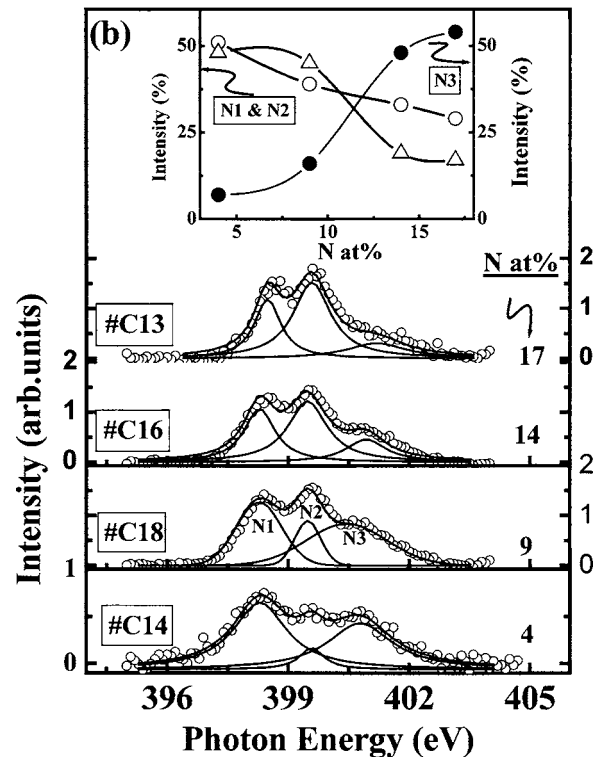
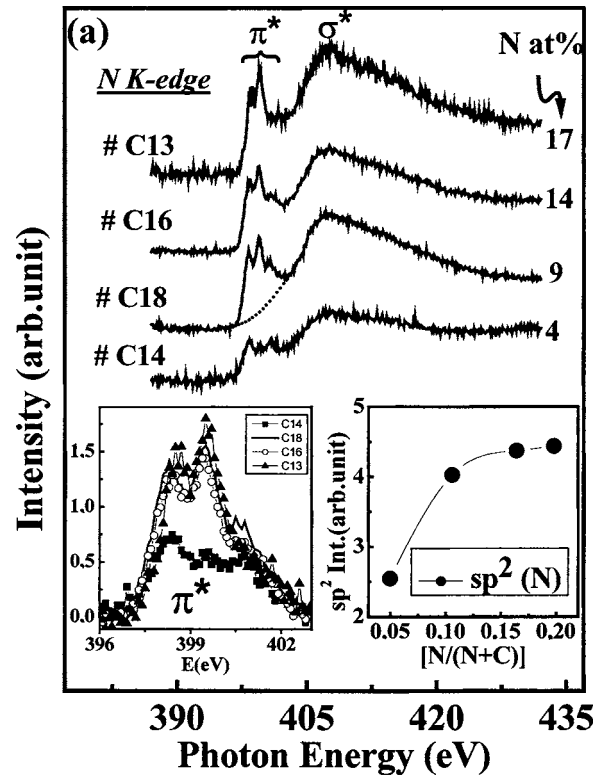


FIG. 2. (a) Normalized N *K*-edge absorption spectra of the *a*-CN<sub>x</sub> films. The inset shows the  $\pi^*$  region after subtraction using a Gaussian line and  $sp^2$  intensity variation with nitrogen content. (b) Decomposed  $\pi^*$  region of the N *K* edge into three peaks and their intensity variation with nitrogen content.

285.2( $\pm$ 0.1) eV representing the graphite structure<sup>3</sup> of the nitrogenated samples, another peak with  $\pi^*$  character [ $1s \rightarrow \pi^*(e_{2u})$  transition<sup>3</sup>] similar to pyridine (C=N)<sup>3,7</sup> appears at 286.8 eV. For a better understanding of the C *K* edge, the  $\pi^*$  peak is decomposed into three peaks within the region of

281–289 eV. The decomposed fitted results are shown in Fig. 1(b). These results show that the intensity of the peak at 286.8 eV (C3) assigned as pyridinelike (C=N) is increasing with an increase of nitrogen concentration, whereas the summation of 284.0( $\pm 0.2$ ) eV (C1) and 285.2( $\pm 0.1$ ) eV (C2) peak intensities assigned as graphite structure decreases in the film structure, as shown in the inset of Fig. 1(b). The whole  $sp^2$  intensity [see the inset of Fig. 1(a)], obtained from integrating within the range of 281–289 eV after subtracting a Gaussian line mentioned above, increases with nitrogen concentration. In the  $\sigma^*$  region of the C  $K$  edge, wider but significant peaks within the range of 291.0–292.8 eV (centered at  $\sim 291.9$  eV) and 293–308 eV (centered at  $\sim 295.8$  eV) are observed (marked by an arrow and a vertical line, respectively) and they are assigned as  $\sigma^*$  (C=C) and  $\sigma^*$  (C–N and C=N) bonds, respectively.<sup>5,7</sup>

In the case of the N  $K$ -edge spectrum, Fig. 2(a) shows a sharp  $1s \rightarrow \pi^*$  resonance at  $\sim 399.5$  eV (N2), with two other peaks on either sides, at 398.3 eV (N1) and 400.8( $\pm 0.3$ ) eV (N3), which are clearly shown in Fig. 2(b) after decomposition into three peaks. This  $\pi^*$  range is shown in the left inset of Fig. 1(a) after subtracting a Gaussian line. The presence of three peaks in the  $\pi^*$  region are three different chemical environments, which are generally observed in carbon nitride thin films.<sup>9,10</sup> The general shapes of the N  $K$ -edge spectra are the same for all  $CN_x$  films. The relative intensities of the different features, however, differ depending on N at. % presence in the film structure. The sharpness of the peak at 399.5 eV (N2) suggests that it originates from a *well-defined* structure, known as the nitrile structure. Since the nitrile bond predominantly has  $\pi$  character, this peak appears strong in the  $\pi^*$  region and its intensity is increasing with N at. % [see the inset of Fig. 2(b)]. Furthermore, the spectrum of N1 centered at 398.5 eV corresponds to pyridinelike N. Regarding the peak at  $\sim 400.8$  eV (N3), this is assigned to N in substitutional graphite sites in agreement with many authors.<sup>10</sup> The right inset in Fig. 2(a) presents the intensity of the  $\pi^*$  of the N  $K$  edge, as obtained from integrating the area within the range of 396–403 eV. It increases and then saturates at a higher nitrogen content. This can be explained by a transition from nonplanar to planar nitrogen bonding geometry when the composition of one nitrogen atom per ring is approached.<sup>11</sup> It is observed that the intensity of the  $\pi^*$  of the C  $K$  edge increases with nitrogen content [see right inset of Fig. 1(a)], which implies that the formation of an  $a-CN_x$  film depends predominantly on C as well as N. In the  $\sigma^*$  region of the N  $K$  edge, a  $1s \rightarrow \sigma^*$  transition is observed as a broad feature centered at  $\sim 407$  eV which is a superposition of graphitelike and pyridinelike nitrogen structures.<sup>10</sup>

There is abundant theoretical and experimental evidences of a correlation between  $\sigma^*$  resonance energy  $\Delta\sigma$  relative to the ionization potential (IP), and bond length [ $\Delta\sigma = E_\sigma - IP$ ],<sup>12</sup> where  $E_\sigma$  is the  $\sigma^*$  resonance position in eV. To determine the C–N bond lengths, we have used the relation,  $R = 1.33 \text{ \AA} - (0.011 \text{ \AA/eV})\Delta\sigma$ , which is an interpolation of the experimental data on small molecules collected by Stöhr.<sup>12</sup> The average C–N bond length are determined from

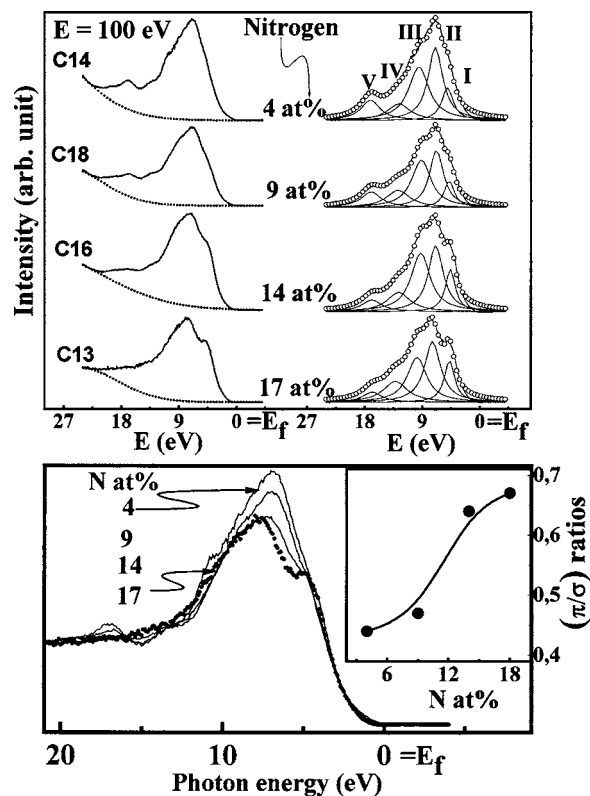


FIG. 3. Valence-band photoelectron spectroscopy (PES) with a Gaussian line for subtraction and decomposed into different peaks. Below shows the normalized spectra and inset ( $\pi/\sigma$ ) intensity ratio with nitrogen content.

the position of the maximum of the  $\sigma^*$  resonance and is  $1.36 \pm 0.01$  Å. The uncertainty margin in these bond lengths is due to the uncertainty in interpolating the formula given above. This bond length suggests predominant  $sp^2$  hybridization because expected  $sp^2$ -hybridized C–N bonds range from 1.40 Å (three carbon neighbors) to 1.33 Å (two carbon neighbors), whereas the  $sp^3$ -hybridized C–N bonds are 1.47 Å.

Figure 3 shows the valence-band PES spectra of films with different at. % of nitrogen ranging from 4- to 17-at. % N. They exhibit a very smooth shape, typical of amorphous materials, and display basically a prominent peak at about 7.0 eV and a shoulder near 4.6 eV that becomes more prominent in higher nitrogen content films. These two peaks are related to the  $p-\sigma$  and  $p-\pi$  contributions to the density of states (DOS), respectively.<sup>13,14</sup> The intensity of the valence-band PES is gradually decreasing with nitrogen content, as clearly observed in Fig. 3 (below).

In order to understand the role of nitrogen in controlling the electronic structure, the valence-band spectra are decomposed into five peaks after subtracting a Gaussian line, as shown in the right column of Fig. 3 (above). These peaks are  $p-\pi$  (peak I),  $p-\sigma$  (peak II), a mixture of  $s$  and  $p$  states (peak III), and  $s$  (peak IV) bands of carbon with positions of about  $\sim 4.6(\pm 0.1)$ ,  $\sim 7.0(\pm 0.2)$ ,  $\sim 9.6(\pm 1)$ , and  $13.4(\pm 0.2)$  eV, respectively.<sup>13</sup> The peak at  $\sim 16.8(\pm 0.2)$  eV (peak V) is a nitrogen-based polymer, as assigned by Bhattacharyya *et al.*<sup>13</sup> It is clearly observed that with nitrogen incorporation

the intensity of  $p$ - $\pi$  contribution is increasing, which implies the formation of larger  $\pi$ -bonded clusters, and a larger defect density. The  $(\pi/\sigma)$  intensity ratios were obtained from integrating the area of peaks I and II and they increase with nitrogen content as shown in the right inset of Fig. 3 (below), indicating that the carbon structure is becoming more graphitic.

#### IV. CONCLUSION

XANES spectroscopy is used to interpret the plausible electronic and bonding structures from the C and N  $K$  edges of  $a$ -CN<sub>*x*</sub> thin films. The contribution from CN bonds and nitrogen in the CN<sub>*x*</sub> films has been separated from the graphite structure. This structure is found to be similar to pyridine. Valence-band PES shows the effect of nitrogen on the spectral shape of the DOS, in particular, the sensitivity of the  $p$ - $\pi$  DOS to the presence of nitrogen. It confirms the role played by the  $\pi$  bonds in controlling the electronic structure of  $a$ -CN<sub>*x*</sub>. The increase of intensity of the  $p$ - $\pi$  with increasing nitrogen content indicates an increase in the defect density and size of the graphitic islands formed by the clustering of  $\pi$  states in aromatic rings.

#### ACKNOWLEDGMENT

One of the authors (WFP) would like to thank the National Science Council (NSC) of the Republic of China for financially supporting this research under Contract No. NSC 93-2112-M032-018.

- <sup>1</sup>A. Y. Liu and M. L. Cohen, *Science* **245**, 841 (1989), and references therein.
- <sup>2</sup>J. H. Kim, D. H. Ahn, Y. H. Kim, and H. K. Baik, *J. Appl. Phys.* **82**, 658 (1997).
- <sup>3</sup>S. Bhattacharyya, M. Lübke, and F. Richter, *J. Appl. Phys.* **88**, 5043 (2000), and references therein.
- <sup>4</sup>F. Alonso, R. Gago, I. Jiménez, C. Gómez-Aleixandre, U. Kreissig, and J. M. Albella, *Diamond Relat. Mater.* **11**, 1161 (2002).
- <sup>5</sup>Ch. Zietzen, F. Wegelin, G. Schönhense, R. Ohr, M. Neuhäuser, and H. Hilgers, *Diamond Relat. Mater.* **11**, 1068 (2002).
- <sup>6</sup>R. McCann, S. S. Roy, P. Papakonstantinou, J. A. McLaughlin, and S. C. Ray, *J. Appl. Phys.* **97**, 073522 (2005).
- <sup>7</sup>R. A. Rosenberg, P. J. Love, and V. Rehn, *Phys. Rev. B* **31**, 2634 (1994).
- <sup>8</sup>S. Anders, J. Diaz, and J. W. Ager III, *Appl. Phys. Lett.* **71**, 3367 (1997).
- <sup>9</sup>J. M. Ripalda *et al.*, *Phys. Rev. B* **60**, R3705 (1999).
- <sup>10</sup>N. Hellgren, J. Guo, C. Sâthe, A. Agui, J. Nordgren, Y. Luo, H. Ågren, and I. E. Sundgren, *Appl. Phys. Lett.* **79**, 4348 (2001).
- <sup>11</sup>I. Jiménez, R. Gago, J. M. Albella, D. Cáceres, and I. Vergara, *Phys. Rev. B* **62**, 4261 (2000).
- <sup>12</sup>J. Stöhr, *NEXAFS Spectroscopy* (Springer, Berlin, 1992).
- <sup>13</sup>S. Bhattacharyya, C. Spaeth, and F. Richter, *J. Appl. Phys.* **89**, 2414 (2001).
- <sup>14</sup>A. Mansour and D. Ugolini, *Phys. Rev. B* **47**, 10201 (2000).